

Journal of Engineering Science and Technology  
Vol. 13, No. 8 (2018) 2464 - 2480  
© School of Engineering, Taylor's University

## LABORATORY EXPERIMENT BASED PERMEABILITY REDUCTION ESTIMATION FOR ENHANCED OIL RECOVERY

AZZA HASHIM ABBAS, WAN ROSLI WAN SULAIMAN\*,  
MOHD ZAIDI JAAFAR, AUGUSTINE AJA AGI

Department of Petroleum Engineering, Faculty of Chemical and Energy Engineering,  
University of Technology Malaysia, Skudai, 81310 Johor, Malaysia

\*Corresponding Author: r-wan@petroleum.utm.my

### Abstract

Formation damage is an unwanted operational problem-taking place through several phases of oil reservoir life. The permeability reduction is a key indicator for the formation damage. Suitable assessment of permeability reduction is critical for hydrocarbon recovery. As oil production reach tertiary recovery stage in many fields, formation damage critical evaluation is needed to avoid additional operational cost and technical feasibility concern. The interaction between reservoir minerals and chemical injection practices is not fully understood. Also, clay mineral presence is highly sensitive to the chemicals, while adsorption phenomena can also occur. The degree of permeability reduction cannot be generalized for core/field scales; therefore investigating the permeability reduction in core scale is important before field-scale assessment. Therefore, this study investigates the permeability reduction after chemicals injection under low flow rate in sand-quartz cores and in the presence of kaolinite. Artificial sandpacks were used to control the sand-kaolinite mixture percentage. The permeability was measured before and after each flood by pressure drop calculation. The study showed that the seawater flood has the highest reduction in permeability followed by polymer and surfactants. Also, the results showed a strong effect of surfactant nature and molecular weight on the adsorption process and consequently the permeability reduction. The study provides an insight for the effect of chemicals on cores physical properties.

Keywords: Enhanced oil recovery, Formation damage, Permeability reduction, Seawater salinity.

## 1. Introduction

Formation damage may define as “a decline in the initial permeability of the reservoir rock following various wellbore operations. Formation damage may be irreversible, which has a serious economic impact on the productivity of the reservoir”. An alternative definition is “a reduction in the initial permeability of the reservoir rock around the wellbore following various operations such as drilling, completion, injection, attempted stimulation or production of the well”. The practical understanding about formation damage and skin effect damage help to describe many good productivity impairments. This also includes any materials that obstruct the normal flow of fluids to the surface. In the Last decades, formation damage aspects were exclusively used to describe obstructions occurring in the near-wellbore region of the rock matrix [1]. However, it is very important to understand the role of formation damage and permeability reduction in the reservoir.

Knowing the correct estimation of permeability is essential for identifying the recoverable hydrocarbon in place accurately. In addition, permeability is one of the main factors of understanding the oil flow. Any reduction in permeability in the reservoir or near the wellbore will affect the flow geometry. Moreover, in some cases when the permeability became low the solid-liquid molecular force will result in nonlinear flow (non-Darcy’s flow). In addition, in certain stages in the reservoir production life, the effect of capillary pressure cannot be ignored, especially in term of EOR projects. According to the relation between capillary tube model and pore radius, any decrease in pore radius will decrease the force in the interface, which, cannot be neglected [2, 3]. The relationship between the interface forces is inversely proportionate to the pore radius.

To address the effect of clay minerals presence on formation damage, the link between the clay minerals (types, fraction, and distribution) with the permeability reduction was studied by several researchers [1, 4-6]. The migrating and pore-plugging characteristics of illite and kaolinite particles after the water injection movement resulted in permeability reduction using SEM [7]. For smectite clays, at saline water injection the particles released can migrate after swelling if it attains a threshold or critical salt concentrations [7]. Zhou et al. [8] tried to determine the exact condition for swelling to occur, the work mainly focused on drilling fluids operations. Montmorillonite was found to reduce the permeability due to fines migration pore blockage [7]. Recently, studies report that kaolinite particles surface charges distribution can result in kaolinite accumulation and blocking the pore throats.

Hydrodynamically, the relation between applying chemical and formation damage was taken seriously after the expansion of Enhanced Oil Recovery (EOR) activities in last decades. However, Zhou et al. [8] reported that some chemical in EOR can cause formation damage. However, previous studies failed to take this into consideration. Few authors tried to describe the effect of EOR on formation damage, however, the reported data were limited to water flooding and polymer flooding [8-11].

An earlier study by Sharma et al. [12] investigated the water flow effect by using combined measurements of core-pressure drop and of suspended-particle concentration in the core outlet, led to quantify the fines migration and its relation with adsorption phenomena. Bedrikovetsky et al. [13] proposed a mathematical model for deep-bed filtration with formation damage coefficient. The study used

laboratory method to determine the formation-damage coefficient from inexpensive and simple pressure-drop measurements by using three-point pressure measurements. A field scale for the Bohai offshore in China showed the effect of water flow on formation damage. The study used two parameters (permeability reduction and rate of wellhead pressure rise) to evaluate the formation damage around injection wells. The data indicated severe formation damage around the wellbore of injection wells, the analysis mainly depended on the pressure performance curve stages that show different characteristics.

Formation damage caused steam injection in sandstone reservoirs was reported by [14]. The authors demonstrated that the injected water stream causes a substitution of the smaller mineral ion within the clay structure. The test results show that three different forms of formation damage as kaolinite transform to swelling smectite clay, wettability alternation, mineral dissolution and re-precipitation. Likewise, another type of steam was investigated by [15], which is a Cyclic Steam Stimulation (CSS). The study used simulated transient pressure test for on-going field operation, they concluded that damage was not as expected and the skin factor near the wellbore was decreasing. Which, they said was because of the overestimation of the data used.

Earlier research showed numerous beneficial effects of injecting alkali or increasing chemical flooding pH to maximize the oil recovery. But Hayatdavoudi and Ghalambor [16] investigated highly kaolinitic sandstone from Tuscaloosa, Louisiana, that had been subjected to sodium hydroxide treatment at pH 10-12. This treatment brought a considerable decrease in permeability, which was attributed to the in-situ conversion of kaolinite booklets to dickite and halloysite. The kaolinite conversion resulted in the disintegration, fragmentation and volume increase of the kaolin mineral within the same pore space. Moreover, studies showed that the alkaline flooding causes the silica dissolution. Also, the soluble amorphous silica allows short-term dissolution rates to be extrapolated to reservoir times. The silica caused a major irreversible permeability reduction. Also, a similar finding was observed regarding the effect of alkali flooding on porous media properties for both permeability and porosity [17, 18].

Additionally, the polymer, which considered as a heavy molecular weight molecules is used in EOR to prevent excess water flow or increasing the water viscosity [19]. However, polymers tend to adsorb a thin layer on the rock surface and the adsorption mechanism is usually described by the residual resistance factor [20]. The permeability reduction by polymer has been proven on both field and core scales. The effect was not limited to low permeability, it affected the high and moderate ranges. This formation damage is irreversible [21]. However, the results are not consistent with the estimated range of permeability reduction. The observations also proved severe plugging in the near wellbore [22]. In the case of low to moderate permeability, after the adsorption occurs, the boundary effect may become dominant [3]. If the adsorption reduces the permeable zones to the size of the pore throat, the fluid flow will be restricted and it needs to overcome the surface molecule force and consequently, the threshold pressure affects the fluid flow [23, 24]. Despite the use of models to describe the effect of polymer on all the permeability ranges, the role of clay minerals was not studied extensively and its effect in the tight pores. Yee et al. [11] studied the effect of Alkaline-Surfactant and Polymer (ASP); they reported that the overall chemical EOR slugs are a risk to

formation damage. However, they did not find a direct link between surfactant flooding and permeability reduction.

Through all the literature, the clay mineral migrates as a consequence of physical or chemical reaction, which, has proven to be a direct cause of permeability reduction, especially during hydrodynamic flow [25]. However, kaolinite mineral behaviour is not fully understood especially at laboratory scale. In some cases, the presence of kaolinite had been observed to reduce the permeability while in other experiments the reduction was not observed [26].

Therefore, it is necessary to understand the compositional flow limitation, by estimating the permeability reduction. The risk factor of permeability reduction may diminish the feasibility of chemicals applicability in heterogeneous reservoirs and it has not been carefully considered in previous studies. The correct estimation of permeability reduction can help in avoiding overestimation of recovery factor despite the source of calculation. In general, the information obtained from permeability reduction in core scale is significant for planning the EOR projects in oil fields. Therefore, this study will answer the following questions that are been asked in EOR.

- What is the rank order of permeability reduction between the injected chemicals under the same flow rate in sand-quartz cores and in presence of kaolinite?
- Thus, surfactant molecular weight has an impact on the permeability reduction.
- Which chemical is the least to cause the formation damage experimentally?

Thus, this study is aimed at estimating the permeability reduction experimentally. Whereas, estimating the reduction in cores containing kaolinite is necessary to understand the role of kaolinite in permeability reduction since a consensus has not been reached.

## **2. Methodology**

### **2.1. Chemicals**

Anionic surfactant Sodium Dodecyl Sulfate (SDS) and Gemini surfactant Aerosol-OT Dioctylsulfonate sodium salt (96% purity) were used for this study. The surfactant was purchased from Acros Organics. The polymeric alkali lignin was purchased from Sigma Aldrich, the molecular weight was approximately 10000 g/mol. Sodium chloride, NaCl was purchased from across the company with a molecular weight of 58.44 g mol<sup>-1</sup> and purity of 99.99%. The quartz sand was collected from Teluk Ramunia, Johor, and kaolinite was purchased from Sigma Aldrich in grade *K*. The entire chemicals used were of analytical grade and was used without further purification.

### **2.2. Preparation of chemical solutions**

The standard brine solution was prepared in a standard 1000 mL volumetric flask. The weight in the mass of 35 g NaCl surfactant is taken and emptied into the volumetric flask, and then distilled water was used to complete the solution to obtain the required weight (1 kg). Finally, all chemicals were prepared in a concentration of 1 wt.%. All the chemical were adjusted to have a pH of 7.

### 2.3. Sand pack and porous media preparation

The sand packs preparation was made in two steps preparing the rock samples and porous media preparation.

#### 2.3.1. Rock sample preparation

The rock samples used in this study are kaolinite and quartz sand, the rock minerals were crushed using a rock pulverizer (BICO, Incorporated) to make the sample finer. The samples were then passed through USA Standard Testing Sieves, ATM Corporation, New Berlin, Wisconsin. The rock samples were air-dried for 24 hours and oven dried at 105°C for 24 hours, these samples were used in both the batch and displacement experiment. About 5 g of each sample was taken for morphological analysis and another 5 g of each sample were further crushed to get a fine particle for X-Ray Diffraction (XRD) analysis.

#### 2.3.2. Porous media preparation

Porous media used in this study experiments was a PVC tube with an inner diameter (*ID*) of 3.4 cm and a length of 31 cm. To achieve a homogeneous compaction of the sand pack, while simultaneously shaking, Deionized Water (DIW) was added from the top of the pipe and the sand compacted. The vacuum pump was used to extract the water from the bottom of the pipe after packing was complete. To prevent the fine grains movement a micron filter of 40 microns was used to block both endings. The mixture of the quartz sand was 98% to 2% kaolinite and it was aged for 60 days before further use. The ageing process was extended long enough to obtain consolidate cores and to settle the kaolinite in the pores.

### 2.4. Characterization technique

The X-Ray Diffraction (XRD) analysis was done using a SIEMENS D500 with *Cu K $\alpha$*  radiation,  $\lambda=0.15147$  nm, at a voltage of 40 kV and current of 200 mA, the scattered radiation was spotted at an angular range of 5-60° ( $2\theta$ ), with a scanning speed of 1 deg/min. The SEM/EDX analysis was performed using Philips XL 40 with an acceleration of 20 kV at the required magnification. The samples were placed on the sample holder followed by a 1-minute sputter coating of gold.

### 2.5. Permeability test

The sand packs were saturated with DIW from the bottom using a strainer pump. DIW was injected and passed through the sand packs to assure a homogenous DIW saturation of the porous media. Then, the saturated sand packs were weighed. The difference in weight before and after saturation is the weight of the DIW. With reference to the DIW density (1 g/cc), the volume of DIW that represents the porous media pore volume ( $V_p$ ) was calculated. The porosities of the sand packs were measured by dividing  $V_p$  to the sand packs bulk volumes ( $V_b$ ).

where:

$W_1$ =weight of vacuumed and dried sandpack (g)

$W_2$ =weight of saturated sandpack (g)

$W_{DIW}=W_2-W_1$ = weight of saturated water in sandpack (g) (1)

$h$ =sandpack length (cm)

$r$ =inside sandpack radius (cm)

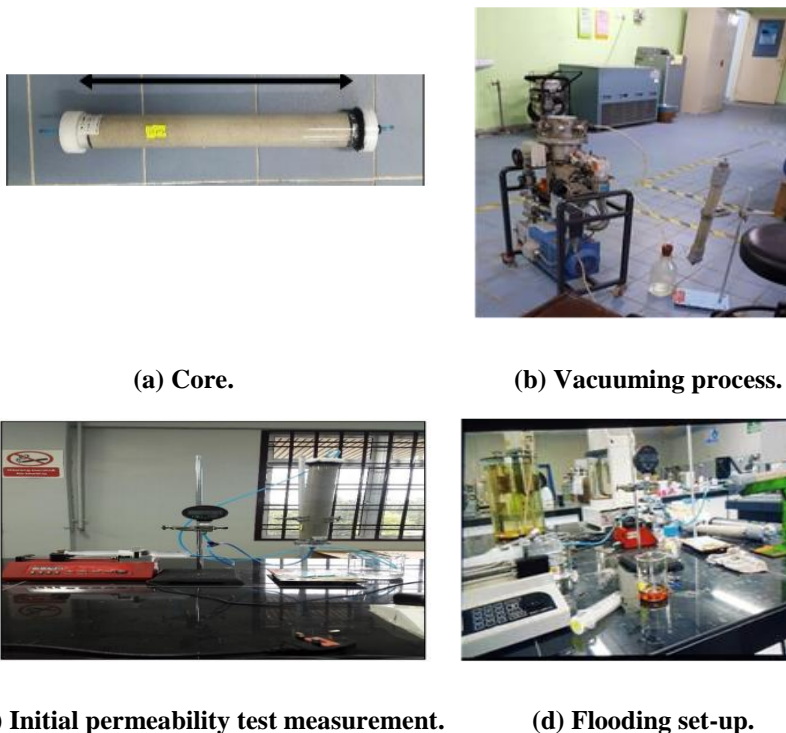
$$\rho_{DIW} = \frac{W_{DIW}}{V_p} \quad (2)$$

$$V_p = \frac{W_{DIW}}{\rho_{DIW}} \quad (3)$$

$$V_b = \pi r^2 h \quad (4)$$

$$\Phi = \frac{V_p}{V_b} \quad (5)$$

The permeability of the sand pack was measured before and after flooding. Vertical upward flow direction was selected in order to determine the permeability of the sand pack. For horizontal permeability the sand pack was positioned horizontally, the horizontal position represents the real reservoir flow direction. The permeability test setup is presented in Fig. 1.



(a) Core.

(b) Vacuuming process.

(c) Initial permeability test measurement.

(d) Flooding set-up.

**Fig. 1. Experiment setup.**

The permeability of porous media was calculated by measuring the pressure difference along the holders at different flow rates (1 mL/min to 5 mL/min). The selected flow rates were used because it is in the range of laminar flow and the flow rate remains proportional to the pressure gradient.

$$k = \frac{q\mu l}{A\Delta P} \quad (6)$$

where:

$k$ =permeability (Darcy)

$q$ =flow rate (mL/s) (adjusted with syringe pump)

$\mu$ =viscosity of DIW (cp)

$L$ =length of sandpack (cm)

$A$ =surface area of the sand pack (cm<sup>2</sup>)

$\Delta P$ =differential pressure (atm) (obtained from pressure gauge)

### 3. Results and Discussion

#### 3.1. Sand and kaolinite characterization

The X-Ray Diffraction (XRD) result shows the major and minor mineral in each sample. The mineral composition was determined using the area under the graph and the intensity of the peak. Every mineral reflection was detected at a certain wavelength by using the Bragg equation. The quantity of each of the identified mineral was estimated using the peak area. Figure 2 shows the X-ray diffractogram of the powder sample. The single-headed peak indicates that there is no impurity in the sample and only one phase is present. The highest peak for sand was at 26.7 with the intensity of 1250. The clay mineral detection was more difficult since the data sensitivity is in the range of 0 to 15. For kaolinite, the highest peak was in 2-Theta 12.3 (Fig. 3). The results of kaolinite 2-Theta are similar to that obtained by [27, 28] , However, the presence of quartz impurity was dominant in 2-Theta 26 and accordingly the matching software indicated the presence of low quartz impurity [27].

The SEM and EDX results show the percentage of silicon, oxygen and aluminium present in each sample (Figs. 4 and 5).

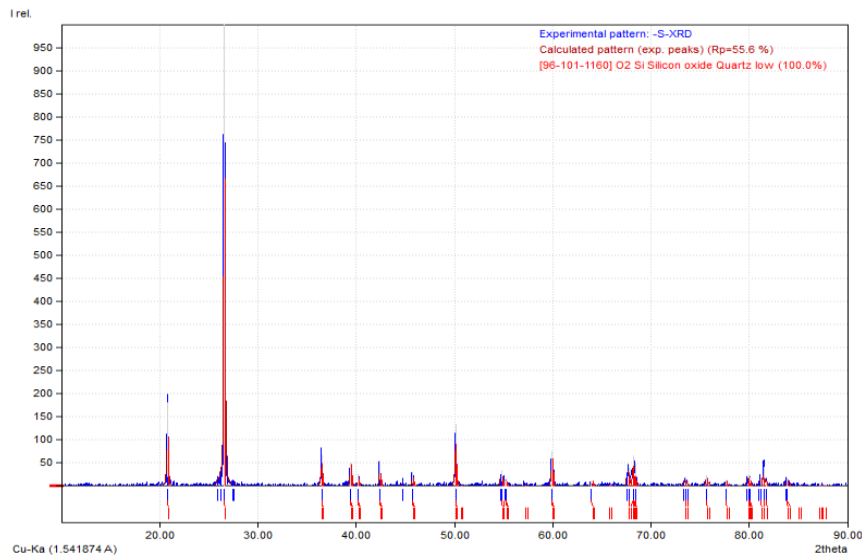


Fig. 2. XRD pattern for sand.

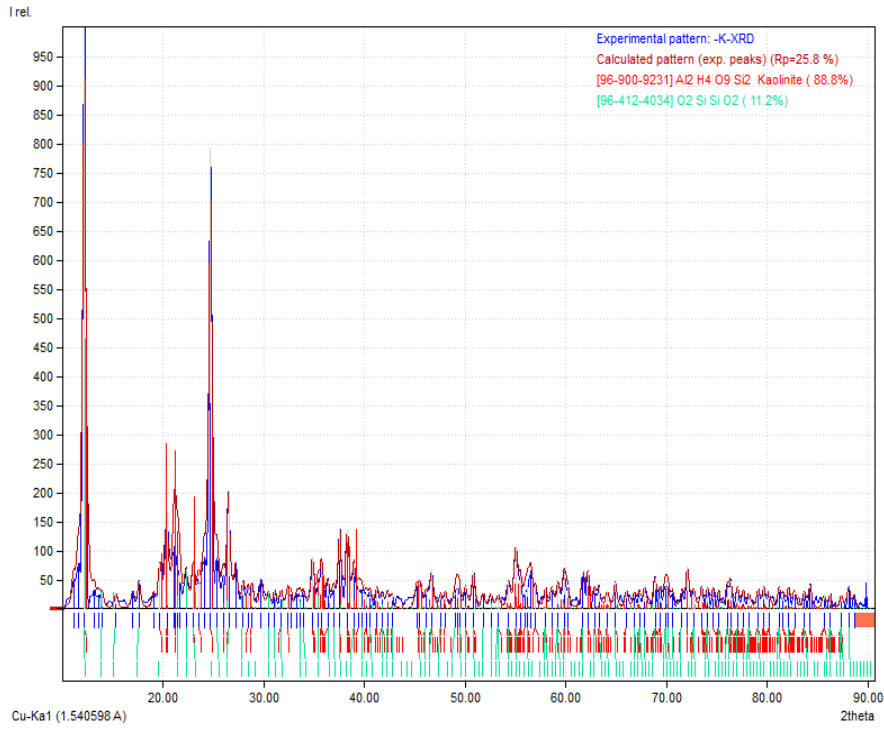
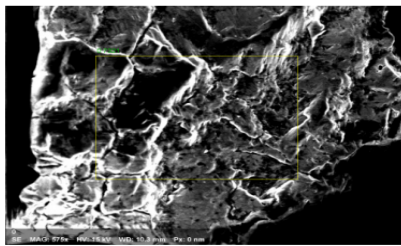


Fig. 3. XRD for kaolinite.



Name Date Time HV Mag WD  
 0 02/05/2017 10:21:23 15.0 keV 575x 10.3 mm

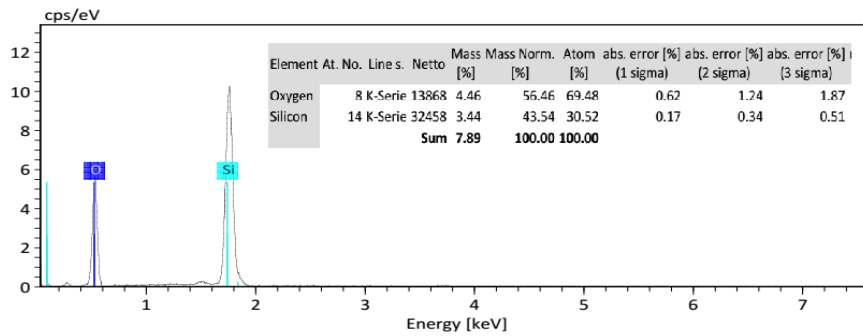


Fig. 4. Sand-SEM and EDX results.



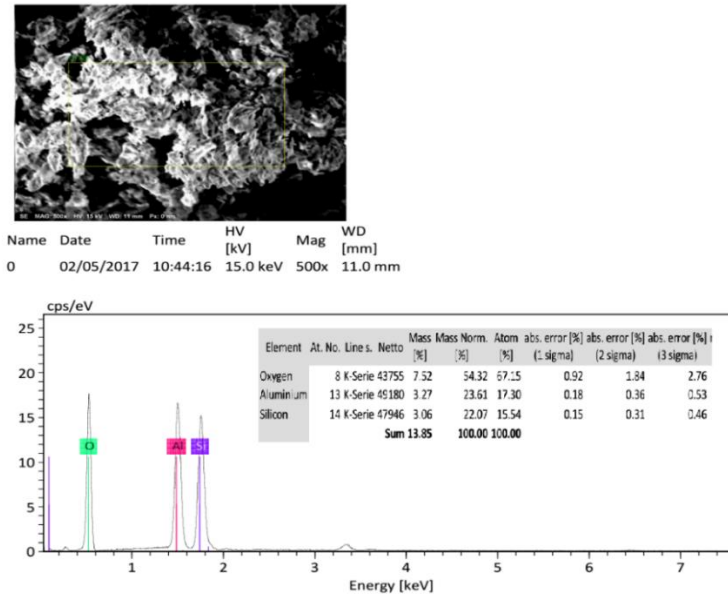


Fig. 5. SEM-EDX of kaolinite.

### 3.2. Permeability test

In these experiments, the cores were prepared and initial properties were measured. The core porosity was calculated before the permeability test. In addition, the horizontal permeability and vertical permeability were measured to validate the sandpack homogeneity. Table 1 shows the result of the pre-flood measurement for all the sandpacks.

Table 1. Sandpack initial properties.

Pack description	Porosity %	Vertical permeability (Darcy)	Horizontal permeability (Darcy)
100% Sand-1	38.5	7.05	9.24
100% Sand-2	38.3	6.48	9.04
100% Sand-3	38.1	6.18	8.4
100% Sand-4	38.7	6.27	9
98% Sand+2% Kaolinite	29.7	1.55	2.78
98% Sand+2% Kaolinite	29.7	1.43	2.55
98% Sand+2% Kaolinite	29.1	1.2	2.3
98% Sand+2% Kaolinite	29.2	1.24	2.1

The porosity results in Table 1 shows moderate porosity for sand cores, the porosity range was higher in absence of kaolinite. The kaolinite presence reduced the porosity up to 23%. Which, agrees with the previous study by Walderhaug [29] who reported that the effect of clay minerals in lowering the porosity.

The horizontal permeability is higher than the vertical according to the packing force direction and it consists with wide range numbers of sandstone reservoir

under the bedding forces [29]. The horizontal permeability and vertical permeability with respect to the compaction stress is shown in Fig. 6.

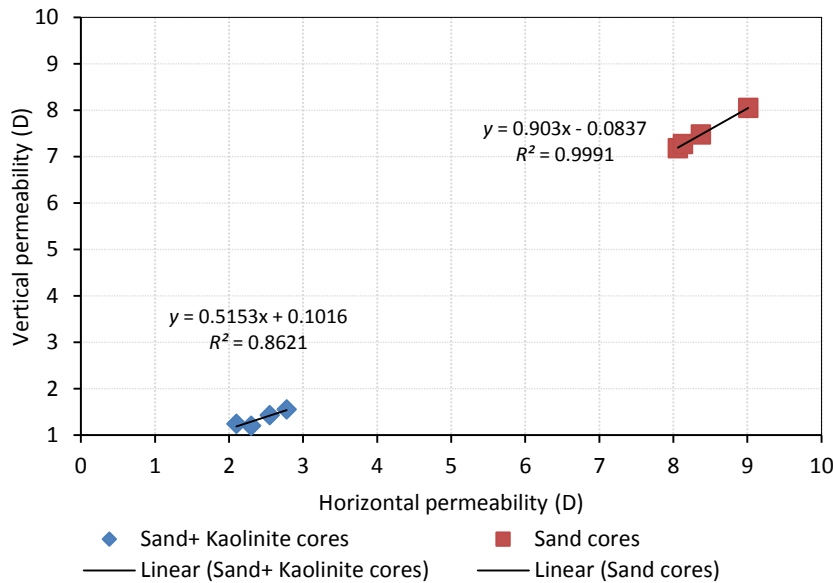


**Fig. 6. Core homogeneity description.**

The horizontal-vertical-permeability relation in Fig. 6, indicates the homogeneous distribution of sand cores. However, the results for sand-kaolinite show moderate distribution. This is because of kaolinite filling in between the sand particles. Clavaud et al. [30] reported that permeability reduced logarithmically with the addition of clay mineral to the synthetic quartz-clay rocks. The sandpack is in the range for isotropy range since the regression coefficient is more than 0.75.

### 3.3. Flooding results

All the cores were injected at 3 PV for each flood. The vertical permeability results after the flood injection are shown in Table 2.

**Table 2. Vertical permeability results after chemical injection.**

Pack description	Porosity %	Vertical permeability (Darcy)
100% Sand-1-Seawater flood	38.5	6.35
100% Sand-2-SDS flood	38.3	6.18
100% Sand-3-Aerosol-OT flood	38.1	6.14
100% Sand-4-Lignin flood	38.7	6.13
98% Sand+2% Kaolinite-seawater flood	29.7	1.37
98% Sand+2% Kaolinite-SDS flood	29.7	1.33
98% Sand+2% Kaolinite-aerosol-OT flood	29.1	1.08
98% Sand+2% Kaolinite-lignin flood	29.2	1.09

The results in Table 2 shows lower permeability compared to the initial properties in Table 1. The results were used to calculate the vertical permeability reduction results in percentage as shown in Figs. 7 and 8.

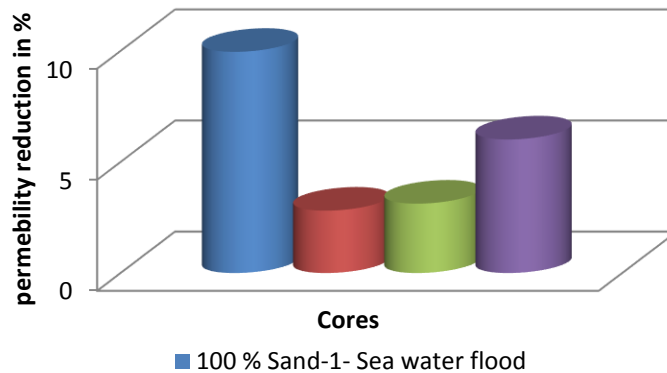


**Fig. 7. Permeability reduction in sand pack floods.**

The results in Fig. 7 shows a high reduction in permeability after seawater flooding. Also, the reduction can be seen for the other flooding however, it was not as high as in the seawater flood sandpacks. The results in Fig. 8 shows a higher reduction in permeability for all the floods. Highest reduction was observed for the group of cores that contains 2% kaolinite. Among all cores, the seawater injected seems to be reducing the permeability, even more than the lignin polymer. The findings indicate a strong influence of chemicals in the presence of kaolinite rather than sand. The aqueous chemistry impact during the flooding resulted in kaolinite particles destabilization. This agrees with previous studies of [21, 31, 32] when they reported the effect of water salinity and polymer on clay minerals.

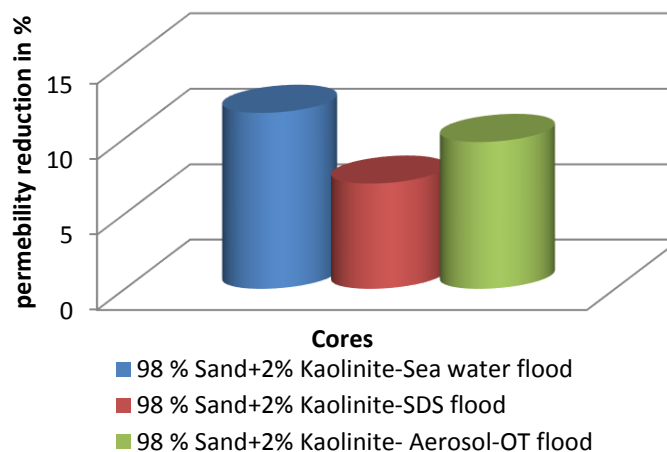


**Fig. 8. Permeability reduction in presence of kaolinite.**

### 3.4. Seawater flood

The results indicate that the permeability reduction in sandpack is 9.9% in sandpack and to 11.6% in presence of kaolinite. The difference is 2% approximately; the results are high, despite a low flow rate. The effect of saline water as a source for permeability reduction could be described by two phenomena. The first is the chemical phenomenon, which is the water sensitivity to sand. The second one is mechanical, which is the particle release by hydrodynamic forces. In this study, the hydrodynamic forces could be ignored since the flow rate used was not high enough and the oil does not exist. The chemical aspect describes the reduction in the presence of salt played a role in silica dissolution, which is in agreement with Islam and Ali [33]. Also, the clay particles released caused migration to occur and induce the pore blockage [32]. The kaolinite release is because of the opposing forces of Van der Waals attraction forces and the repulsive electrostatic forces [12].

### 3.5. Lignin polymer flood

In polymer flooding, lignin was investigated due to several reasons such as its suitability as polymer [33], as part of polymer blends [34] and as a sacrificial agent with the ability to reduce surface tension [35, 36]. Several researchers have reported the ability of lignin to adsorb on the rock surface, which has led to its use for sacrificial agent purposes. The results show the strong influence of lignin on permeability reduction. The reduction in the sand is lower than in presence of kaolinite by 9%. The result indicates the difficulty of the lignin polymer flow path in presence of kaolinite. The ability of lignin to adsorb on the sand surface during the flow is a time-wise process, as long as the period of flow of the lignin is extended. It will form the adsorbed layer and reduce the permeability [37, 38]. Polymer tends to flow through the high permeable zone, which is visible for sand cores more than in kaolinite cores accordingly to the mechanical entrapment [39]. In presence of kaolinite, the adsorption process is as a result of the electrostatic attraction between the side positive charge on the kaolinite surface and the phenol group in lignin. This behaviour is because of the heavy molecules injected was adsorbed, which, led to a reduction in permeability similar result was reported by Hirasaki and Pope [40] and Mishra et al. [41]. Also, the thickness of the adsorbed layer is high, which, also resulted in permeability reduction [42]. This result is important criteria for further understanding the dynamic flow applicability in the range of EOR studies.

### 3.6. Surfactant flood

The surfactants used in this study have different molecular weight and different adsorption rate to minerals. The permeability reduction is higher for Aerosol-OT than SDS; this could be as a result of the hydrophobic effect. Moreover, Aerosol-OT has a tendency to adsorb on the rock surface and forms more viscous micelles [43]. This agrees with previous studies by Atay et al. [44] and Abbas et al. [45] when they reported that SDS adsorbs less on soil and clay minerals. Surfactant effect on pores was observed by Nikpay et al. [46], they reported a change in flow rate and build-up pressure associated with the adsorption. Also, the data showed that during surfactant flood, permeability reduced between (7 to 10%) depending on the surfactant concentration (below or above the critical micelle concentration)

[47]. In the current finding, the reduction was in the range of 4-6% in sand and 8 to 11% in presence of kaolinite.

#### 4. Conclusions

Permeability reduction and formation damage are a known problem for petroleum engineers. Changing the permeability during chemical flood results in altering the flow behaviour also affects the estimated recovery factor. The sensitivity of permeability reduction has been ignored at the reservoir scale and core scale in several studies. Despite the fact that limited studies tried to address polymer retention in porous media or stimulation process near wellbore impact on permeability reduction, this study focused on permeability changes during several chemical flows. This research focused on introducing the sand as the main component of the sandstone reservoir and the kaolinite as a strong adsorbent for chemicals.

This work has revealed that during the core flood the permeability changes are recognizable and cannot be neglected. The finding could be summarized as follows:

- For seawater flood, the permeability reduction was the highest followed by lignin polymer>Aerosol-OT>SDS.
- The presence of kaolinite has a strong impact on permeability reduction. The highest reduction was 11.6% during seawater flow. Whereas, in the absence of kaolinite the permeability reduction was lower.
- The salinity effect on releasing sand particles and the strong interaction with kaolinite was the major cause of the reduction.
- In the study observations, the sand pack flood tests for lignin polymer indicated that lignin could cause high permeability reduction up to 7% even though the flow rate is low. In addition, the reduction may extend to pore plugging level and it is mainly because of the adsorption. The adsorption occurred on both sand and kaolinite surface and it reduced the permeability up to 11% in presence of kaolinite due to the initial sand pack permeability. This happens because of the high molecular weight of the polymer can strongly aggregate in layers on the wall of the pore.
- The results reveal that surfactants flood stimulates the permeability reduction. The range of permeability reduction was between (2% to 5%) in sand cores and (7% to 11%) in kaolinite presence. The current results supported by the role of the surfactant molecular on surfactant adsorption capacity.
- In the study finding, we could conclude that lower molecular surfactant SDS was the least causing of permeability reduction in cores

The study findings have confirmed the role of the chemical in altering the permeability of the core during the flow, which, might help in justifying the difference between lab experimental result and simulated lab result for many researchers. The current study possibly to support the decision-makers in choosing the best chemical implication considering the formation damage. In our suggestions, the permeability alteration studies should be encouraged.

**Nomenclatures**

$A$	Surface area of the sand pack, cm <sup>2</sup>
$k$	Permeability, Darcy
$L$	Length of sandpack, cm
$r$	Sandpack inner radius, cm
$V_b$	Bulk volume, mL
$V_p$	Pore volume, mL

**Greek Symbols**

$2\theta$	Angle between transmitted beam and reflected beam
$\Delta P$	Differential pressure, atm
$\Phi$	Porosity%
$\mu$	Viscosity, cp

**Abbreviations**

DIW	Deionized Water
PVC	Polyvinyl Chloride
XRD	X-Ray Diffraction

**References**

1. Krueger, R.F. (1988). An overview of formation damage and well productivity in oilfield operations: An update. *Proceedings of the SPE California Regional Meeting*. California, 24 pages.
2. Ying'er, D.; Yan, Q.; and Ma, B. (1998). Relationship between interfacial molecular interaction and permeability and its influence on fluid flow. *Petroleum Exploration and Development*, 25, 46-49.
3. Guo, H.; Wang, F.; Li, Y.; Yu, Z.; Gao, X.; YuanyuanGu; Chen, J.; Shasha, F.; and Xinling, Z. (2015). Progress on flow mechanism in low permeability formation. *Procedia Engineering*, 126, 466-470.
4. Bennion, B.D.; Thomas, F.B.; and Sheppard, D.A. (1992). Formation damage due to mineral alteration and wettability changes during hot water and steam injection in clay-bearing sandstone reservoirs. *Proceedings of the Symposium on the SPE Formation Damage Control*. Lafayette, Louisiana, 18 pages.
5. Bedrikovetsky, P.; Vaz, A.S.L.; Furtado, C.J.A.; and de Souza, A.R.S. (2011). Formation-damage evaluation from nonlinear skin growth during coreflooding. *SPE Reservoir Evaluation & Engineering*, 14(2), 193-203.
6. Fang, W.; Jiang, H.; Li, J.; Li, W.; Li, J.; Zhao, L.; and Feng, X. (2016). A new experimental methodology to investigate formation damage in clay-bearing reservoirs. *Journal of Petroleum Science and Engineering*, 143, 226-234.
7. Mohan, K.K.; Reed, M.G.; and Fogler, H.S. (1999). Formation damage in smectitic sandstones by high ionic strength brines. *Colloids and Surfaces a Physicochemical and Engineering Aspects*, 154(3), 249-257.
8. Zhou, Z.; Cameron, S.; Kadatz, B.; and Gunter, W.D. (1997). Clay swelling diagrams: Their applications in formation damage control. *SPE Journal*, 2(2), 99-106.

9. Wilson, M.J.; Wilson, L.; and Patey, I. (2014). The influence of individual clay minerals on formation damage of reservoir sandstones: A critical review with some new insights. *Clay Minerals*, 49(2), 147-164.
10. Arensdorf, J.J.; Kerr, S.; Miner, K.; and Ellis-Toddington, T.T. (2011). Mitigating silicate scale in production wells in an oilfield in Alberta. *Proceedings of the SPE International Symposium on Oilfield Chemistry*. The Woodlands, Texas, United States of America, 5 pages.
11. Yee, H.V.; Halim, N.H.B.; Salleh, I.K.B.; Hamid, P.B.A.; and Sedaralit, M.F.B. (2013). Managing Chemical EOR (ASP) effects on formation damage and flow assurance in malay basin, Malaysia. *Proceedings of the International Petroleum Technology Conference*. Beijing, China, 2869-2875.
12. Sharma, M.; Shutong, P.; Wennberg, K.E.; and Morgenthaler, L.N. (1997). Injectivity decline in water injection wells: An offshore Gulf of Mexico case study. *SPE Production and Facilities*, 15(1), 6-13.
13. Bedrikovetsky, P.; Siquerra, F.D.; Furtado, C.J.A.; and de Souza, A.L.S. (2011). Modified particle detachment model for colloidal transport in porous media. *Transport in Porous Media*, 86(2), 353-383.
14. Yang, S.; Sheng, Z.; Liu, W.; Song, Z.; Wu, M.; and Zhang, J. (2008). Evaluation and prevention of formation damage in offshore sandstone reservoirs in China. *Petroleum Science*, 5(4), 340-347.
15. Sulaiman, W.R.W.; and Hashim, A. (2016). Cyclic steam stimulation effect on skin factor reviewed case study. *Applied Mechanics and Materials*, 818, 287-290.
16. Hayatdavoudi, A.; and Ghalambor A. (1996). Controlling formation damage caused by kaolinite clay minerals: Part I. *Proceedings of the SPE Formation Damage Control Symposium*. Lafayette, Louisiana, 7 pages.
17. Southwick, J.G. (1985). Solubility of silica in alkaline solutions: Implications for alkaline flooding. *Society of Petroleum Engineers Journal*, 25(6), 857-864.
18. Beckingham, L.E.; Peters, C.A.; Um, W.; Jones, K.W.; and Lindquist, W.B. (2012). Changes in the pore network structure of Hanford sediment after reaction with caustic tank wastes. *Journal of Contaminant Hydrology*, 131(1-4), 89-99.
19. Li, Z.; Zhang, W.; Tang, Y.; Li, B.; Song, Z.; and Hou, J. (2016). Formation damage during alkaline-surfactant-polymer flooding in the Sanan-5 block of the Daqing Oilfield, China. *Journal of Natural Gas Science and Engineering*, 35, 826-835.
20. Agi, A.; Junin, R.; Gbonhinbor, J.; and Onyekonwu, M. (2018). Natural polymer flow behaviour in porous media for enhanced oil recovery applications: A review. *Journal of Petroleum Exploration and Production Technology*, 1-14.
21. Gan, L.; Zhou, M.; Yang, D.; and Qiu, X. (2014). Adsorption characteristics of carboxymethylated lignin at a hydrophobic solid/water interface. *Iranian Polymer Journal*, 23(1), 47-52.
22. Lai, N.; Qin, X.; Ye, Z.; Li, C.; Chen, K.; and Zhang, Y. (2013). The study on permeability reduction performance of a hyperbranched polymer in high permeability porous medium. *Journal of Petroleum Science and Engineering*, 112, 198-205.

23. Treiber, L.E.; and Yang, S.H. (1986). The nature of polymer plugging and a wellbore treatment to minimize it. *Proceedings of the Symposium on the SPE Enhanced Oil Recovery*. Tulsa, Oklahoma, 11 pages.
24. Sheng, J.J. (2016). Formation damage in chemical enhanced oil recovery processes. *Asia-Pacific Journal of Chemical Engineering*, 11(6), 826-835.
25. Pang, Z.; Li, J.; Shi, S.; Li, Y.; Liu, H.; Chen, J.; Zhang, F.; and Zhang, Z. (1998). Effect of polymer molecular weight on residual permeability reduction factor. *Proceedings of the Symposium on Chemical Flooding Research Results during the Eighth Five-Year Period (1991-1995)*. Beijing, 138-149.
26. Wilson, L.; Wilson, M.J.; Green, J.; and Patey, I. (2014). The influence of clay mineralogy on formation damage in North Sea reservoir sandstones: A review with illustrative examples. *Earth-Science Reviews*, 134, 70-80.
27. Rosenbrand, E.; Fabricius I.L.; and Yuan, H. (2012). Thermally induced permeability reduction due to particle migration in sandstones: The effect of temperature on kaolinite mobilisation and aggregation. *Proceedings of the Thirty-Seventh Workshop on Geothermal Reservoir Engineering*. Stanford, California, 10 pages.
28. Menking, K.M.; Musler, H.M.; Fitts, J.P.; Bischoff, J.L.; and Andersen, R.S. (1993). Clay mineralogical analyses of the Owens Lake core. *U.S. Geological Survey, Open-File Report 93-683*. Core OL-92, Owens Lake, Southeast California.
29. Walderhaug, O. (1996). Kinetic modelling of quartz cementation and porosity loss in deeply buried sandstone reservoirs. *AAPG Bulletin*, 80(5), 731-745.
30. Clavaud, J.-B.; Mainault, A.; Zamora, M.; Rasolofosaon, P.; and Schlitter, C. (2008). Permeability anisotropy and its relations with porous medium structure. *Journal of Geophysical Research: Solid Earth*, 113(B1), 1-10.
31. Barnaji, M.J.; Pourafshary, P.; and Rasaie, M.R. (2016). Visual investigation of the effects of clay minerals on enhancement of oil recovery by low salinity water flooding. *Fuel*, 184, 826-835.
32. Saha, R.; Uppaluri, R.V.S.; and Tiwari, P. (2017). Effect of mineralogy on the adsorption characteristics of surfactant-reservoir rock system. *Colloids and Surfaces A: Physicochemical and Engineering Aspects*, 531, 121-132.
33. Islam, M.R.; and Ali, S.M.F. (1989). New scaling criteria for polymer, emulsion and foam flooding experiments. *Journal of Canadian Petroleum Technology*, 28(4), 10 pages.
34. Kia, S.F.; Fogler, H.S.; and Reed, M.G. (1987). Effect of salt composition on clay release in berea sandstones. *Proceedings of the SPE International Symposium on Oilfield Chemistry*. San Antonio, Texas, 10 pages.
35. Ek, M.; Gellerstedt, G.; and Henriksson, G. (2007). *Pulp and paper chemistry and technology (Volume 2)*. Sweden: KTH Royal Institute of Technology.
36. Kun, D.; and Pukánszky, B. (2017). Polymer/lignin blends: Interactions, properties, applications. *European Polymer Journal*, 93, 618-641.
37. Wei-qing, W.; Guang-yu, X.; and Yu-peng, Z. (2001). The application of modified alkali lignin as sacrificial agent in tertiary oil recovery. *Journal of Hunan University (Natural Science)*, 2, 21-26.



38. Chen, S.; Shen, S.; Yan, X.; Mi, J.; Wang, G.; Zhang, J.; and Zhou, Y. (2016). Synthesis of surfactants from alkali lignin for enhanced oil recovery. *Journal of Dispersion Science and Technology*, 37(11), 1574-1580.
39. Bai, Y.; Li, J.; Zhou, J.; and Li, Q. (2008). Sensitivity analysis of the dimensionless parameters in scaling a polymer flooding reservoir. *Transport in Porous Media*, 73(1), 21-37.
40. Hirasaki, G.J.; and Pope, G. (1974). Analysis of factors influencing mobility and adsorption in the flow of polymer solution through porous media. *Society of Petroleum Engineers Journal*, 14(4), 337-346.
41. Mishra, S.; Bera, A.; and Mandal, A. (2014). Effect of polymer adsorption on permeability reduction in enhanced oil recovery. *Journal of Petroleum Engineering*, 9 pages.
42. Farajzadeh, R.; Bedrikovetsky, P.; Lotfoliahi, M.; and Lake, L.W. (2016). Simultaneous sorption and mechanical entrapment during polymer flow through porous media. *Water Resources Research*, 52(3), 2279-2298.
43. Al-Hashmi, A.R.; and Luckham, P.F. (2010). Characterization of the adsorption of high molecular weight non-ionic and cationic polyacrylamide on glass from aqueous solutions using modified atomic force microscopy. *Colloids and Surfaces A: Physicochemical and Engineering Aspects*, 358(1-3), 142-148.
44. Atay, N.Z.; Yenigün, O.; and Asutay, M. (2002). Sorption of anionic surfactants SDS, AOT and cationic surfactant Hyamine 1622 on natural soils. *Water, Air, and Soil Pollution*, 136(1-4), 55-68.
45. Abbas, A.H.; Sulaiman, W.R.W.; Jaafar, M.Z.; and Aja, A.A. (2017). Micelle formation of aerosol-OT surfactants in seawater salinity. *Arabian Journal for Science and Engineering*, 43(5), 2515-2519.
46. Nikpay, M.; Lazik, D.; and Krebs, P. (2015). Water displacement by surfactant solution: An experimental study to represent wastewater loss from sewers to saturated soil. *International Journal of Environmental Science and Technology*, 12(8), 2447-2454.
47. Nikpay, M.; Lazik, D.; and Krebs, P. (2015). Permeability changes by surfactant solution: An experimental study to represent wastewater loss from sewers to saturated soil. *Environmental Earth Sciences*, 73(12), 8443-8450.